

Magnetotunneling Studies of the Dimensionality of the Emitter Electron Gas of Double Barrier Devices

B. R. A. Neves, E. S. Alves, J. F. Sampaio and A. G. Oliveira

*Departamento de Física, Instituto de Ciências Exatas, Universidade Federal de Minas Gerais
Caixa Postal 702, 30161-970 Belo Horizonte, MG, Brasil*

and

E. A. Meneses

Instituto de Física, Universidade Estadual de Campinas, Campinas, SP, Brasil

Received July 12, 1993

We use magnetotunneling measurements to investigate the dimensionality of the electron gas in the emitter region of a double barrier device (DBD) under bias. The electron gas in the emitter of a DBD may have a two- or a three-dimensional character and, depending on its nature: the selection rules for tunneling predict different behavior on the $I(V)$ characteristics of the devices. We investigate a series of n-type GaAs/(AlGa)As DBD with varying emitter doping profile in order to determine its influence on the emitter electron gas dimensionality. We show that the electron gas has a two-dimensional character for lightly doped emitter layers ($2 \times 10^{16} \text{ cm}^{-3}$) and it has a three-dimensional nature for a high nominal doping ($2 \times 10^{18} \text{ cm}^{-3}$). For intermediary doping levels ($2 \times 10^{17} \text{ cm}^{-3}$) there is evidence for both a 2D and a 3D electron gases depending on the applied bias.

I. Introduction

Recently there has been great interest in magnetotunneling studies of GaAs/(AlGa)As double barrier devices (DBD) due to their potential application as high speed devices and also because their electrical properties are controlled by fundamental quantum processes. Magnetotunneling measurements have been widely used to investigate the quantum properties of the emitter electron gas of DBD^[1-4] and also to analyze the dimensionality of the emitter states, which is determined mainly by the conduction band profile and the doping in the contact region. However, in spite of the importance of the nature of the emitter states for the shape of the current-voltage characteristics of DBD and, consequently, to device performance, no systematic study has been done to determine the influence of the doping profile on the dimensionality of the emitter electron gas. In this work we report magnetotunneling measurements carried out on a series of

GaAs/(AlGa)As DBD with varying doping in the contacts and use the data to determine the nature of the emitter states.

In the sequential picture^[5], tunneling in an ideal DBD is governed by conservation of both energy and transverse momentum (i.e. momentum perpendicular to the tunneling direction). It has been demonstrated that in real devices scattering mechanisms such as those involving longitudinal optical phonons, ionized impurities or surface roughness, break the momentum conservation condition and, in this case, tunneling is controlled only by conservation of energy^[3,6]. A magnetic field applied parallel to the tunneling direction quantizes the emitter density of states into Landau levels but does not change the selection rules (conservation of transverse momentum is equivalent to conservation of the Landau-level index). However, the field causes different effects on the $I(V)$ characteristics of a DBD depending on whether the emitter electron gas has a two-dimensional (2D) or a three-dimensional (3D) char-

acter.

In a DBD with a heavily doped emitter contact, the electrons tunnel from degenerate 3D states to empty 2D states in the well. When a bias is applied to a device charge accumulates at the emitter barrier and the potential is modified producing a band bending in the accumulation region which is highly sensitive to the emitter doping profile. A low doping level in this region leads to the formation of a quasi-two-dimensional bound state in the accumulation potential when the device is biased and a two-dimensional electron gas (2DEG) is formed adjacent to the emitter barrier.

The structures investigated in this work were grown by molecular beam epitaxy (MBE) and consisted of the following layers in order of growth from the n^+ - Si doped (100) oriented GaAs substrate: (i) 1 μm of GaAs, Si doped to $n = 2 \times 10^{18} \text{ cm}^{-3}$; (ii) 500 \AA of GaAs, with nominal doping $n = N_e$; (iii) GaAs spacer of thickness t ; (iv) 56 \AA of $\text{Al}_{0.4}\text{Ga}_{0.6}\text{As}$; (v) 120 \AA of GaAs well; (vi) 56 \AA of $\text{Al}_{0.4}\text{Ga}_{0.6}\text{As}$ barrier; (vii) GaAs spacer of thickness t' ; (viii) 500 \AA of GaAs, with nominal doping $n = N'_e$; (ix) 1 μm of GaAs, Si doped to $n = 2 \times 10^{18} \text{ cm}^{-3}$. The well and the barriers were undoped, as were the spacer layers intended to prevent diffusion of dopants into the active layers. The samples were processed by using standard photolithographic techniques into 100 μm diameter mesas, and ohmic contacts were made by alloying Au-Ge-Ni at 400 $^\circ\text{C}$ for 30 seconds in a 15:85% $\text{H}_2:\text{N}_2$ atmosphere. The $I(V)$ measurements were carried out at liquid-helium temperature using the pseudo-four-probe technique with a variable DC voltage source. Depending on the polarity of the applied bias, electrons can tunnel either from the top to the substrate contact or in the opposite direction. As the top and bottom contact layers have different doping profiles by reversing the polarity of the applied voltage to the device the electrons will tunnel from emitters which have different characteristics. The doping N_e (or N'_e) and the thicknesses t (or t') of the emitter side of the devices are listed in table 1.

Table 1 - Effect of the spacer layer thickness and emitter doping level on the dimensionality of the emitter electron gas of a DBD.

Emitter	Doping level $N_e \text{ (cm}^{-3}\text{)}$	Spacer-layer thickness $t \text{ (\AA)}$	Electron-gas dimensionality
A	2×10^{16}	25	2D
B	2×10^{16}	50	2D
C	2×10^{16}	75	2D
D	2×10^{17}	12	2D-3D
E	2×10^{17}	25	2D-3D
F	2×10^{17}	50	2D-3D
G	2×10^{18}	25	3D

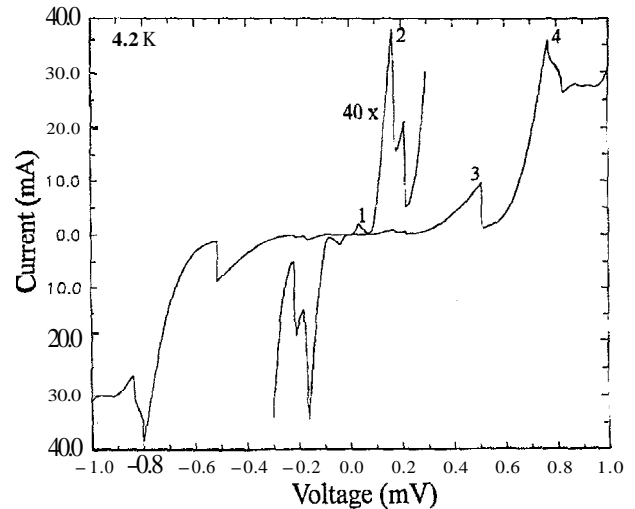


Figure 1: Current-voltage characteristics at 4.2 K of a symmetric structure with the emitter doped to $N_e = 2 \times 10^{16} \text{ cm}^{-3}$ and a 25 \AA emitter spacer. The resonant peaks are labeled 1-4.

A typical $I(V)$ curve at zero magnetic field is shown in Fig. 1 for a device with emitter characteristic A (see table 1). Four resonant peaks are clearly seen and are labeled 1-4 in the figure. The features beyond the fourth peak in both forward and reverse bias are due to phonon-assisted tunneling^[3,6]. This is the only symmetric structure investigated and this is reflected in the symmetry of the $I(V)$ curve in the two bias polarities (positive bias corresponds to the flow of electrons from the substrate to the top layer). All devices show four peaks in the current-voltage characteristics and we have investigated the emitter-electron-gas dimensionality in the voltage range corresponding to each peak.

Figures 2 and 3 show the conductance versus applied bias for structures with emitter characteristics C and E,

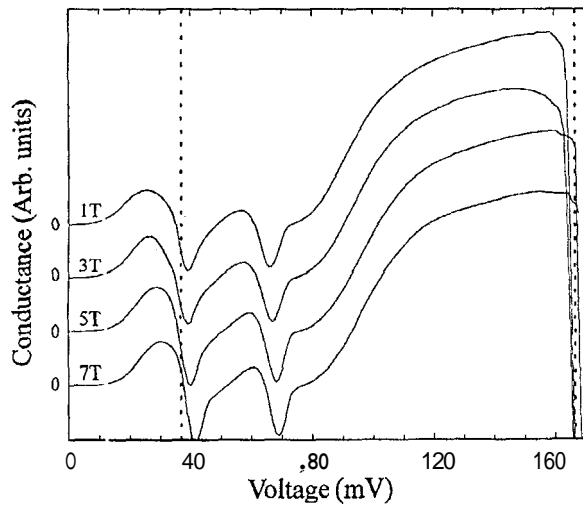


Figure 2: Conductance vs. voltage of a DBD with emitter E (see Table 1) at several magnetic fields ($B||J$) at 4.2 K. The dotted lines indicate the position of the resonant peaks. The absence of oscillations below the resonances is evidence of a 2DEG in the emitter.

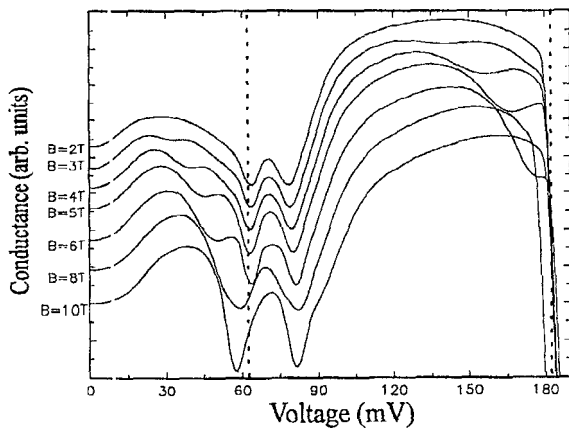


Figure 3: Conductance vs. voltage of a DBD with the emitter doped to $N_e = 2 \times 10^{17} \text{ cm}^{-3}$ and a 25 \AA spacer (see Table 1) at several parallel magnetic fields. The dotted lines show the positions of the main resonant peaks. The oscillations seen before the resonances indicate the 3D nature of the emitter states.

respectively, for several values of magnetic fields ($B||J$) in the voltage range corresponding to the first and second resonances. The positions of the resonant peaks are indicated in the figure by dotted lines. The magnetic field produces oscillations in the conductance dI/dV of device E (see Fig. 3), in the voltage region below the resonant peaks. As the magnetic field is increased, the oscillations move to higher bias and become stronger and the spacing between them increases linearly with field. We have not observed any oscillation in the conductance of the structure with lower doping and larger spacer in the emitter (Fig. 2), in the presence of a magnetic field.

These magnetotunneling features can be understood by considering the selection rules for tunneling from a 2D- or a 3D-electron gas into the 2D-states of the well, in the presence of a magnetic field. When a bias is applied across a DBD, electrons accumulate in the region adjacent to the emitter barrier. A low doping level in this region can enhance the band bending causing spatial quantization of the electrons in the accumulation layer, as shown in Fig. 4(a). This figure shows a schematic band diagram for a DBD biased on resonance, i.e. when the quasi-bound state in the emitter accumulation potential is at the same energy as the well state. A qualitative representation of this situation is illustrated in the energy-transverse momentum space diagram shown in Fig. 4(b). At zero field the two-dimensional emitter states are represented in this space by a paraboloid filled up to the Fermi energy and the well states are represented by an empty paraboloid. At zero bias the emitter paraboloid is below the quasi-bound state in the well and resonant tunneling cannot occur. As the bias is increased, the well paraboloid moves down wards relative to the emitter state and the resonance condition is reached when both paraboloids coincide. Tunneling is then possible because both energy and momentum conservation rules are fulfilled. If space charge buildup in the well is neglected, resonant tunneling can occur at only one value of applied bias

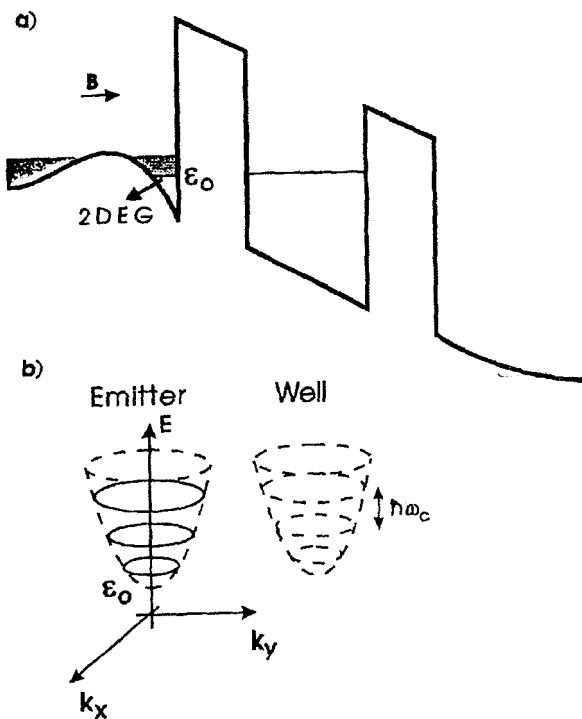


Figure 4: a) Schematic conduction band diagram of a DBD under an applied bias. A 2DEG is formed in the low-doped emitter contact. b) Energy versus transverse-momentum representation of tunneling from a 2DEG in the presence of a magnetic field. Both the emitter and well quasi-bound states are quantized into Landau levels, shown as disks separated by $\hbar\omega_c$. Resonant tunneling occurs at an applied bias such that both emitter and well paraboloids coincide.

and any further increase in bias produces a sharp drop in the current. A magnetic field applied parallel to the current direction further quantizes the emitter and well quasi-bound states into degenerate Landau levels which are separated in energy by $\hbar\omega_c$, where $\omega_c = eB/m^*$ is the cyclotron frequency and m^* is the electron effective mass. The emitter (well) states are represented in Fig. 4(b) by solid (dashed) disks. In the absence of scattering, the transverse momentum must be conserved, therefore magnetotunneling proceeds with conservation of Landau level index, i.e. an electron in the n -th Landau level in the emitter can only tunnel to the n -th Landau level in the well and resonant tunneling occurs at only one value of bias. Thus, when a 2DEG is formed in the emitter of a DBD, no oscillations are expected in the $I(V)$ characteristics of the device in a B field.

The conduction band diagram for a structure with a three-dimensional emitter electron gas is illustrated

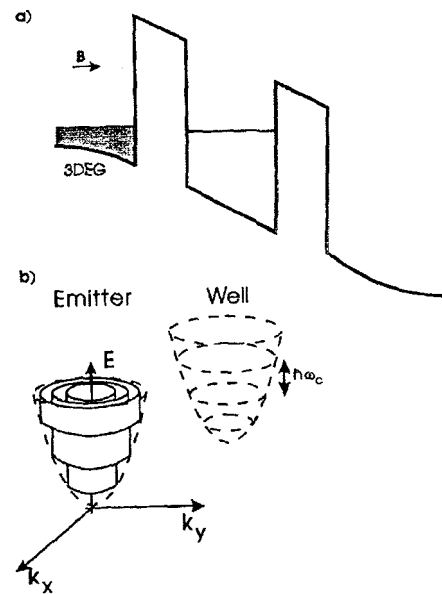


Figure 5: a) Conduction band diagram of a DBD with a heavily doped emitter contact under bias. The three-dimensional emitter states are filled up to the Fermi energy. b) Energy versus momentum representation of tunneling from a 3D emitter electron-gas in a magnetic field. The emitter density of states is quantized into Landau cylinders and tunneling occurs when a well state (dashed disk) passes through the emitter cylinder of the same index, causing oscillations in the current.

in Fig. 5(a) at an applied bias corresponding to the onset of resonance (well state lined up with the emitter Fermi energy E_F). Figure 5(b) shows a schematic illustration of tunneling from 3D emitter states, which are represented in the energy-momentum diagram by a paraboloid filled up to the Fermi energy. Resonant tunneling starts at an applied bias such that the bottom of the well curve intercepts the higher energy emitter states. As bias is swept, more electrons are available to tunnel elastically and the current increases until the well state lines up with the bottom of the conduction band in the emitter. In the diagram this corresponds to the overlap of the emitter and well paraboloids. A further increase in bias makes the current drop sharply. A magnetic field applied parallel to the current quantizes the 3D-states in the emitter into Landau cylinders, as shown schematically in Fig. 5(b). As the applied bias is increased, due to conservation of Landau index the tunneling current should increase in steps as the n -th Landau disk in the well intercepts the n -th Landau cylinder in the emitter. By sweeping bias, additional tunneling

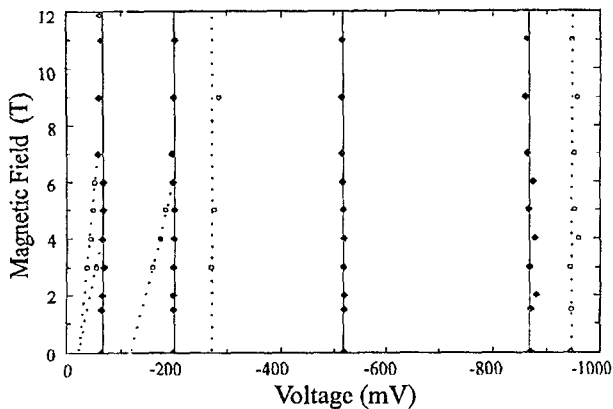


Figure 6: Far diagram showing the voltage positions of the resonances (full squares) and oscillation maxima (empty circles) as a function of magnetic field for a device with emitter F (see Table 1). The vertical dotted lines show the peaks associated with LO-phonon assisted tunneling.^[3] The oscillations observed at voltages below the first and second resonances (empty circles) are associated to tunneling from magnetic-field quantized 3D emitter states.

channels become available in energy steps of $\hbar\omega_c$ until the first Landau well-state pass through the bottom of the first Landau cylinder and the current falls abruptly.

Thus, the observation of current oscillations in the $I(V)$ (or dI/dV) curves is a clear indication of magnetotunneling from a 3D emitter electron gas into a 2D density of states. Therefore we can attribute the oscillations observed in the conductance curves shown in Fig. 3 as tunneling from Landau quantized three-dimensional electronic states in the emitter. Due to the low doping level in the emitter of the device C (see Fig. 2), a 2DEG is formed in the accumulation layer and no oscillation is seen in the conductance in an applied B field. The position of the resonant peaks and of all the oscillations observed in the conductance of the DBD in a magnetic field can be plotted in a $B(V)$ fan diagram as the one shown in Fig. 6 for the device with emitter F. The full squares indicate the voltage position of the four main resonant peaks and are joined by vertical solid lines. The vertical dotted lines indicate the position of the features due to LO-phonon assisted tunneling, which become more evident at higher magnetic fields^[3]. Neither the main peaks nor the LO-phonon peaks move with field. The subsidiary maxima below the main resonant peaks shift to higher bias as the ap-

plied field is increased and are shown as empty circles in the figure. The absence of similar oscillations below the third and fourth peaks is an indication of tunneling from a 2DEG in the emitter. Thus, as the applied bias is increased, the band bending in the emitter accumulation layer grows stronger and a quasi-bound state is formed. Electrons which at low bias are in higher energy 3D emitter states, at higher bias scatter into the lower energy 2D quasi-bound state thermalizing and forming a 2DEG. Similar behavior has been found in the conductance of all devices with an intermediate doping level ($\sim 2 \times 10^{17} \text{ cm}^{-3}$) in the emitter. The dimensionality of the emitter electron gas determined from the magnetotunneling measurements is shown in Table 1 for all devices investigated. We have found evidence for a 2DEG in the emitter of all devices with low nominal doping level ($\sim 10^{16} \text{ cm}^{-3}$) in the contact layers, independent on the spacer thickness. Devices with a heavily doped emitter ($\sim 10^{18} \text{ cm}^{-3}$) contact have a 3D electron gas in the emitter. The magnetotunneling measurements for the three devices with an intermediary nominal doping level ($\sim 10^{17} \text{ cm}^{-3}$) (see Table 1) in the emitter showed evidence for both a 2D and 3D emitter electron gas. A 3D character is found at low applied bias and a 2DEG is observed at higher biases. The band bending in the emitter at low bias is not strong enough to form a quasi-bound level in the accumulation layer, but as the applied bias increases, the band bending also increases, leading to the formation of a quasi-bound state in the accumulation layer, thus lowering the dimensionality of the emitter density of states.

In conclusion, we have carried out magnetotunneling measurements in a series of GaAs/(AlGa)As-based double barrier devices in order to investigate the influence of the emitter doping profile on the dimensionality of the emitter electron gas. The emitter nominal doping and the spacer layer thickness were the only varying parameters in the series of devices studied. We showed that for low nominal doping ($\sim 2 \times 10^{16} \text{ cm}^{-3}$), the

emitter electron gas has always a 2D nature, independent of the spacer layer thickness and of the applied bias. For intermediary doping levels ($\sim 2 \times 10^{17} \text{ cm}^{-3}$) in the emitter, a 3D electron gas is present at low bias and, at higher bias, a 2DEG is formed in the emitter. Finally, for a high nominal doping in the emitter ($\sim 2 \times 10^{18} \text{ cm}^{-3}$), 3D electron gas is present independent on the applied bias. The results were explained in terms of the conduction band bending dependence on the doping profile and on the applied bias.

Acknowledgements

This work was partially supported by CNPq, FINEP and FAPEMIG.

References

1. E. E. Mendez, L. Esaki and W. I. Wang, *Phys. Rev. B* **33**, 2593 (1986).
2. C. A. Payling, C. R. H. White, L. Eaves, E. S. Alves, M. L. Leadbeater, J. C. Portal, P. D. Hodson, D. J. Robins, R. H. Wallis, J. I. Davis and A. C. Marshall, *Superlattices and Microstructures* **6**, 193 (1989).
3. M. L. Leadbeater, E. S. Alves, L. Eaves, M. Henini, O. H. Hughes, A. C. Celeste, J. C. Portal, G. Hill and M. A. Pate, *Phys. Rev. B* **39**, 3438 (1989).
4. A. Zaslavsky, D. C. Tsui, M. Santos and M. Shayegan, *Phys. Rev. B* **40**, 9529 (1989).
5. S. Luryi, *Appl. Phys. Lett.* **47**, 490 (1985).
6. V. J. Goldman, D. C. Tsui and J. E. Cunningham, *Phys. Rev. B* **36**, 7635 (1987).